Article

Environmental Compatibility and Genome Flexibility of *Klebsiella oxytoca* Isolated from Eight Species of Aquatic Animals

Shuo Sun [1,2], Tingting Gu [1,2], Yafei Ou [1,2], Yongjie Wang [1,2], Lu Xie [3] and Lanming Chen [1,2,*]

1   Key Laboratory of Quality and Safety Risk Assessment for Aquatic Products on Storage and Preservation (Shanghai), Ministry of Agriculture and Rural Affairs of China, Shanghai 201306, China
2   College of Food Science and Technology, Shanghai Ocean University, Shanghai 201306, China
3   Institute for Genome and Bioinformatics, Shanghai Institute for Biomedical and Pharmaceutical Technologies, Fudan University, Shanghai 201203, China
*   Correspondence: lmchen@shou.edu.cn

Abstract: *Klebsiella oxytoca* is an emerging pathogen that can cause life-threatening infectious diseases in humans. Recently, we firstly reported for the first time the presence of *K. oxytoca* in edible aquatic animals. In this study, we further investigated its bacterial environmental fitness and genome evolution signatures. The results revealed that *K. oxytoca* isolates ($n = 8$), originating from eight species of aquatic animals, were capable of growing under a broad spectrum of environmental conditions (pH 4.5–8.5, 0.5–6.5% NaCl), with different biofilm formation and swimming mobility profiles. The genome sequences of the *K. oxytoca* isolates were determined (5.84–6.02 Mb, 55.07–56.06% GC content). Strikingly, numerous putative mobile genetic elements (MGEs), particularly genomic islands (GIs, $n = 105$) and prophages ($n = 24$), were found in the *K. oxytoca* genomes, which provided the bacterium with specific adaptation traits, such as resistance, virulence, and material metabolism. Interestingly, the identified prophage-related clusters were derived from *Burkholderia* spp., *Enterobacter* spp., *Klebsiella* spp., *Pseudomonas* spp., and *Haemophilus* spp., suggesting phage transmission across *Klebsiella* and the other four genera. Many strain-specific ($n = 10$–447) genes were present in the *K. oxytoca* genomes, whereas the CRISPR-Cas protein-encoding gene was absent, indicating likely active horizontal gene transfer (HGT) and considerable genome variation in *K. oxytoca* evolution. Overall, the results of this study are the first to demonstrate the environmental compatibility and genome flexibility of *K. oxytoca* of aquatic animal origins.

Keywords: *Klebsiella oxytoca*; genome evolution; virulence; antibiotic and heavy metal resistance; aquatic product; food safety

1. Introduction

Klebsiella oxytoca was first isolated from a specimen of sour milk in 1886. The organism was classified as a member of the genus *Klebsiella* in 1963 [1]. *K. oxytoca* has been implicated in human infectious diseases, including diarrhea [2], ventriculitis [3], keratitis [4], antibiotic-associated hemorrhagic colitis [5], necrotizing enterocolitis [6], bacteremia [7], meningitis [8], spontaneous spondylodiscitis [9], and pyogenic liver abscess [10]. The bacterium also infects other organs, leading to pneumonia as well as urinary tract and skin infections [2].

Antibiotics such as β-lactam drugs can effectively control *K. oxytoca* infection [11]. Nevertheless, due to the inappropriate use of antimicrobials, the increasing resistance of pathogenic bacteria poses an alarming health threat and complicates options for clinical therapy [12]. Antibiotic-resistant *K. oxytoca* isolates have also been reported. For instance, Yang et al. [13] analyzed 5724 *K. oxytoca* clinical isolates from North America ($n = 3501$), Europe ($n = 1783$), the Asia–West Pacific region ($n = 257$), and Latin America ($n = 183$) reported in 2013–2019. They found that the rates of resistance to carbapenems, ceftriaxone, ciprofloxacin (CIP), colistin, and tigecycline were 1.8%, 12.5%, 7.1%, 0.8%, and 0.1%,

respectively. Resistance to carbapenems was increasingly alarming [13]. To the best of our knowledge, reports in the current literature on *K. oxytoca* isolates of environmental or aquatic animal origins are rare. Recently, Abdurehman Damissie et al. [14] isolated and identified *Klebsiella* species in the gut of honey bees collected from worker honey bees (*Apis mellifera*) on Haramaya University bee farm in March–October of 2021 in Ethiopia. *K. oxytoca* was identified from 23.3% of the isolates (*n* = 60). The *K. oxytoca* isolates (*n* = 14) were resistant to ampicillin (54.5%), erythromycin (54.5%), and gentamycin and amoxicillin (18.2%) [14]. In our recent research, *K. oxytoca* was for the first time found in 14 species of aquatic animals, which were sampled in July–September of 2018–2019 in Shanghai, and Fuzhou, China. Approximately 8.0% of the *K. oxytoca* isolates (*n* = 125) displayed multidrug-resistant (MDR) phenotypes [15].

K. oxytoca is a Gram-negative bacterium and inhabits water and soil environments [16], where diverse microbial communities exist as well as pools of naturally occurring antibiotic resistance genes (ARGs). This facilitates rapid antibiotic resistance transmission via horizontal gene transfer (HGT) [17]. Previous studies have also indicated co-selection between antibiotics and heavy metals [18], due to the increasing heavy metal pollution in these environments [19]. For instance, we found that high percentages of the *K. oxytoca* isolates (*n* = 125) in aquatic animals tolerated the heavy metals Cu^{2+} (84.8%), Pb^{2+} (80.8%), Cr^{3+} (66.4%), Zn^{2+} (66.4%), and Hg^{2+} (49.6%) [15].

Currently, complete genome sequences of over 34 *K. oxytoca* isolates are available in the National Center for Biotechnology Information (NCBI) genome database (https://www.ncbi.nlm.nih.gov/, accessed on 1 October 2023). Of these, most strains were isolated from human specimens (*n* = 27), and only a few from the environment (*n* = 4). In this study, based on our recent research findings [15], we further investigated the environmental fitness and genome evolution signatures of *K. oxytoca* isolates originating from eight species of aquatic animals. The major objectives of this study were (1) to characterize the survival traits of the *K. oxytoca* isolates (*n* = 8) under different environmental conditions; (2) to determine the genome sequences of the *K. oxytoca* isolates and identify mobile genetic elements (MGEs) and virulence- and resistance-related genes in the *K. oxytoca* genomes; and (3) to analyze the phylogenetic relationships of the *K. oxytoca* isolates. The results of this study will fill prior gaps in the *K. oxytoca* genomes of aquatic animal origins and improve our understanding of the evolution and pathogenesis of the emerging pathogen worldwide.

2. Materials and Methods

2.1. K. oxytoca Isolates and Cultural Conditions

K. oxytoca strains 7-7-27, 8-2-3-6, 8-2-11, 8-3-38, 8-6-19, 8-8-40 8-1-12-7, and 8-11-1 were isolated from six species of crustaceans (*Mytilus eduli*, *Sinonovacula constricta*, *Scapharca subcrenata*, *Arca granosa*, *Neptunea cumingi Crosse*, and *Anodonta woodiana*); one species of shellfish (*Procambarus clarkia*); and one species of fish (*Carassius auratus*), respectively [15]. The *K. oxytoca* isolates (Supplementary Materials: Table S1) were identified in our recent report [15], and were stored in a −80 °C freezer in the laboratory of Shanghai Ocean University, Shanghai, China. The *K. oxytoca* isolates were routinely incubated in tryptic soybean broth (TSB) medium (pH 7.2, 0.5% NaCl) (Beijing Land Bridge Technology, Beijing, China) aerobically at 37 °C with shaking at 175 rpm [15].

2.2. Antibiotic Susceptibility and Heavy Metal Tolerance Assays

Antibiotic susceptibility of the *K. oxytoca* isolates was determined according to the disco diffusion method approved by Clinical and Laboratory Standards Institute (CLSI, M100-S28, 2018, USA) [15,20]. Mueller–Hinton (MH) agar medium and antibiotic discs were purchased from OXOID, Basingstoke, UK [15,20]. Heavy metal tolerance of the *K. oxytoca* isolates was examined according to broth dilution testing (microdilution, CLSI) [15,20,21]. $CdCl_2$, $CrCl_3$, $CuCl_2$, $HgCl_2$, $MnCl_2$, $NiCl_2$, $PbCl_2$, and $ZnCl_2$ (3200–3.125 µg/mL, Analytical Reagent) were purchased from Sinopharm Chemical Reagent Co., Ltd., Shanghai, China. *Escherichia*

coli ATCC25922 and K12 strains (Institute of Industrial Microbiology, Shanghai, China) were used as quality control strains [15,20,21].

2.3. Growth Curve Assay

Growth curves of the *K. oxytoca* isolates were individually determined at different NaCl concentrations (0.5%, 2.5%, 4.5%, 6.5%, 8.5%) in the TSB medium (pH 7.2), or at different pH values (3.5, 4.5, 5.5, 6.5, 7.5, 8.5) in the TSB (0.5% NaCl) at 37 °C for 24 h, using a Multimode Microplate Reader (BioTek Instruments, Winooski, VT, USA) [18,22].

2.4. Swimming Mobility Analysis

The *K. oxytoca* isolates were individually incubated in the TSB medium (pH 8.5, 0.5% NaCl) at 37 °C until the logarithmic growth stage (LGS). The bacterial culture was inoculated onto semi-solid TSB agar plates (0.5% NaCl, pH 8.5, 0.25% agar). The agar plates were cultured at 37 °C for 72 h. The colony diameters were measured and photographed to analyze the swimming mobility of the *K. oxytoca* isolates [23].

2.5. Biofilm Formation Analysis

Biofilm formation was examined using the crystal violet staining method as described in our recent report [23]. Briefly, the bacterial cell culture at the LGS was inoculated into 24-well bacterial culture plates (1 mL/well), and cultured at 37 °C for 72 h, fixed and stained using the crystal violet, and eluted with 95% ethanol every 12 h. The absorbance values at OD_{600} were measured using the Multimode Microplate Reader (BioTek Instruments, Winooski, VT, USA), and calculated [23].

2.6. Genome Sequencing, Assembly, and Annotation

Genomic DNA of the *K. oxytoca* isolates was individually extracted using a TIANamp Bacteria DNA Kit (Tiangen Biochemical Technology Co., Ltd., Beijing, China) according to the manufacture's instruction. The quality and quantity of the DNA samples for genome sequencing were controlled as described in our recent reports [18,22,23].

Genomes of the *K. oxytoca* isolates were sequenced by Shanghai Majorbio Bio-Pharm Technology Co., Ltd., Shanghai, China, using the Illumina Hiseq × 10 (Illumina, San Diego, CA, USA) platform. Three separately produced DNA samples were used for each of the *K. oxytoca* isolates. Sequence assembly, gene prediction, and Clusters of Orthologous Groups (COG) of proteins were employed using the same software as described in our recent reports [18,22,23] with default parameters. The Virulence Factor database (http://www.mgc.ac.cn/VFs, accessed on 1 October 2023) and ARGs database (http://arpcard.Mcmaster.ca, accessed on 1 October 2023) were used to detect virulence- and resistance-related genes, respectively, via the cloud platform of Shanghai Majorbio Bio-Pharm Technology Co., Ltd., Shanghai, China [18,22].

2.7. Comparative Genome Analysis

MGEs, including genomic islands (GIs), prophages, integrons (Ins), and insertion sequences (ISs), as well as CRISPR-Cas sequences, were predicted in the *K. oxytoca* genomes using the same software as described in our recent reports [18,22] with default parameters. Core genes shared by the eight *K. oxytoca* isolates, and strain-specific genes in single genomes, were predicted using the same software with default parameters [18,22].

A phylogenetic tree was constructed on the basis of 42 *K. oxytoca* isolates, of which the complete genome sequences of 34 *K. oxytoca* isolates are available in the NCBI GenBank database so far. To generate the phylogenomic tree, 1482 single-copy orthologues present in all the genomes were inferred using the OrthoFinder software (version 2.5.5) (https://doi.org/10.1186/s13059-019-1832-y, 19 October 2023). Each sequence of single-copy orthologues was aligned separately using the mafft software (version 7.520) (https://doi.org/10.1093/bioinformatics/bty121, 19 October 2023). Alignments were concatenated via Perl script (https://github.com/nylander/catfasta2phyml, 19 October 2023), and a

maximum likelihood tree (1000 bootstraps) was constructed using the IQ-Tree software (version 2.2.3) (https://doi.org/10.1093/molbev/msaa015, 19 October 2023). Similarly, a phylogenetic tree was constructed on the basis of the identified prophage sequences using the MEGA software (https://www.megasoftware.net, 11 December 2023).

Multilocus sequence typing (MLST) analysis of the *K. oxytoca* isolates was performed on the seven conserved core genes (*gapA*, *infB*, *mdh*, *pgi*, *phoE*, *rpoB*, *and tonB*) in *K. oxytoca* against the MLST database (https://cge.food.dtu.dk/services/MLST/, accessed on 1 October 2023) [20]

2.8. Statistical Analysis

The SPSS software (version 17.0, SPSS Inc., Chicago, IL, USA) was used to analyze the data. All tests were conducted in triplicate.

3. Results and Discussion

3.1. Growth of the K. oxytoca Isolates in Different NaCl and pH Conditions

K. oxytoca 7-7-27, 8-1-12-7, 8-2-3-6, 8-2-11, 8-3-38, 8-6-19, 8-8-40, and 8-11-1 isolates were recovered from eight species of edible aquatic animals, including *M. edulis*, *P. clarkii*, *S. constricta*, *S. subcrenata*, *A. granosa*, *N. cumingi Crosse*, *C. auratus*, and *C. auratus*, respectively (Table S1). The 16S rRNA gene sequencing and analysis confirmed the *K. oxytoca* strains, whose sequences were deposited in the NCBI GenBank database (Table S1).

The bacterial hosts *P. clarkii*, *C. auratus*, and *A. woodiana* were produced in freshwater, while *M. edulis*, *A. granosa*, *N. cumingi Crosse*, *S. constricta*, and *S. subcrenata* were produced in seawater. Therefore, we examined the growth of the *K. oxytoca* isolates at different NaCl concentrations (0.5–8.5% NaCl) in the TSB (pH 7.2) at 37 °C, and the results are illustrated in Figure 1 and Supplementary Figure S1. All the *K. oxytoca* isolates were fully inhibited at 8.5% NaCl; however, they were all capable of growing at 6.5% NaCl, but with a retardation phase (RP) of 4–7 h. Under the 4.5–0.5% NaCl conditions, the *K. oxytoca* isolates grew vigorously, but reached the maximum biomass at 0.5% NaCl (OD_{600} = 1.4).
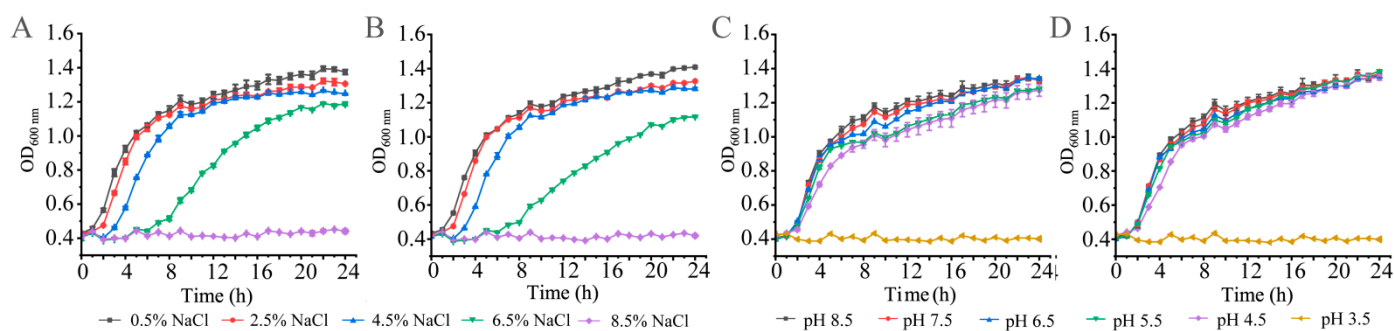

Figure 1. Growth curves of the representative *K. oxytoca* isolates of aquatic animal origins under different concentrations of NaCl and pH conditions. (**A**,**C**) *K. oxytoca* 7-7-27; (**B**,**D**) *K. oxytoca* 8-11-1.

The human acidic stomach environment is a defense barrier that does not allow pathogenic bacteria to pass through. Nevertheless, current studies on the acid or alkaline adaptation of *K. oxytoca* are rare. Therefore, in this study, the growth of *K. oxytoca* isolates was also examined in different pH conditions (pH 3.5–8.5) in the TSB (0.5% NaCl) at 37 °C. As shown in Figure 1 and Supplementary Figure S2, although the growth of all the isolates was completely inhibited at pH 3.5, remarkably, the isolates were all able to grow well in acidic pH 4.5–6.5 conditions. Moreover, under alkaline conditions (pH 7.5–8.5), all the *K. oxytoca* isolates grew vigorously, as well, and reached maximum biomass at pH 8.5, with the OD_{600} values ranging from 1.31 to 1.45.

The results of this study provide the first experimental evidence for a broad spectrum of pH (4.5–8.5) conditions under which *K. oxytoca* isolates of aquatic animal origins were capable of survival. Moreover, the *K. oxytoca* isolates were all capable of growing vigorously

at 0.5–6.5% NaCl. Most recently, we reported the growth traits of *Klebsiella pneumoniae* isolates recovered from seven species of commonly consumed aquatic animals, including *M. veneriformis*, *Cipangopaludina cahayensis*, *T. granosa*, *Eriocheir sinensis*, *P. clarkii*, *Epinephelus fuscoguttatus*, and *Misgurnus anguillicaudatus* [18]. These *K. pneumoniae* isolates were found to be able to grow at pH 4.5–7.5 and 0.5–1.0% NaCl in the TSB at 37 °C [18]. Compared with these, the results of this study highlight wide ranges of saline concentrations (0.5–6.5%) and pH (4.5–8.5) in which *K. oxytoca* isolates originating from aquatic animals were capable of survival, indicating their notable compatibility and fitness in their niches.

3.2. Biofilm Formation of K. oxytoca Isolates of Aquatic Animal Origins

A biofilm is a population of bacterial cells growing on a surface and is enclosed in an exopolysaccharide matrix. Biofilm formation allows bacteria to survive in hostile environments and colonize in new niches [24]. Therefore, in this study, for the first time, we examined the biofilm formation dynamics of *K. oxytoca* isolates of aquatic animal origins (Figure 2).
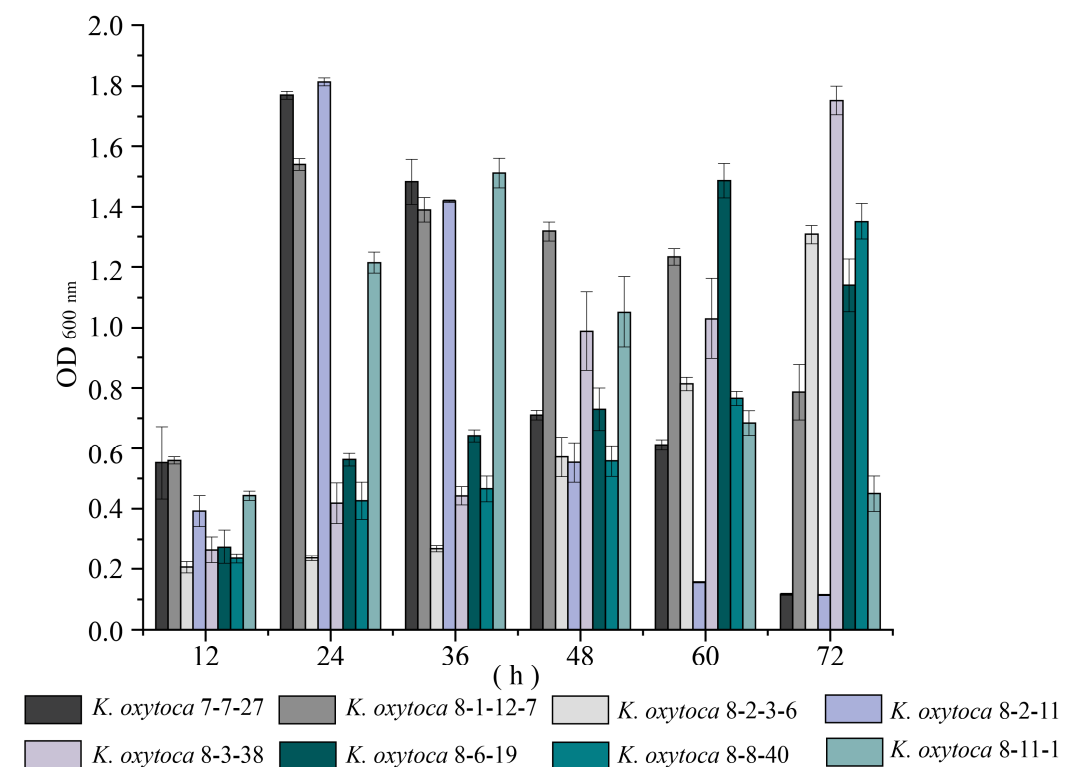

Figure 2. Biofilm formation of *K. oxytoca* isolates of aquatic animal origins. The *K. oxytoca* 7-7-27, 8-1-12-7, 8-2-3-6, 8-2-11, 8-3-38, 8-6-19, 8-8-40, and 8-11-1 isolates were incubated in the TSB (pH 8.5, 0.5% NaCl) at 37 °C for 72 h.

As shown in Figure 2, the isolates displayed distinct biofilm formation dynamics. For example, the biofilm of *K. oxytoca* 7-7-27, 8-1-12-7, and 8-2-11 isolates developed rapidly, and reached their maximum biomass at 24 h; then, they decreased sharply at 48 h. Conversely, the biofilm formation of *K. oxytoca* 8-2-3-6, 8-3-38, and 8-8-40 isolates was relatively slower, reaching their maximum biomass at 72 h. Among all the isolates, *K. oxytoca* 8-2-11 from *S. subcrenata* showed the strongest ability to form a biofilm with the highest production at 24 h (OD_{600} = 1.81). It will be interesting to investigate its potential virulence in future research.

3.3. Swimming Mobility of K. oxytoca Isolates of Aquatic Animal Origins

Motility is involved in the interaction between microorganisms and their host, specifically in colonization or infectious pathogenic processes [25]. Therefore, we examined the

swimming motility of the *K. oxytoca* isolates in the TSB (pH 8.5, 0.5% NaCl, 0.25% agar) at 37 °C for 72 h (Supplementary Materials: Figure S3).

As shown in Figure S3, swimming motility differed among the *K. oxytoca* isolates. For example, *K. oxytoca* 8-3-38 from *A. granosa* displayed maximum swimming diameters of 8 mm, 15.5 mm, and 21 mm at 24 h, 48 h, and 72 h, respectively. In contrast, *K. oxytoca* 8-8-40 swam the most slowly, with swimming diameters of 5.5 mm, 9 mm, and 10 mm at 24 h, 48 h, and 72 h, respectively, which were 0.69-fold, 0.58-fold, and 0.48-fold smaller than those of *K. oxytoca* 8-3-38.

3.4. Genome Features of K. oxytoca Isolates of Aquatic Animal Origins

Based on the obtained results, we further determined draft genome sequences of the eight *K. oxytoca* isolates using the Illumina Hiseq × 10 sequencing platform, which generated 20,195–204,452 clean single reads. The sequence assembly generated 34–90 scaffolds. The obtained genome sizes were in the range of 5,837,340–6,018,771 bp with GC contents of 55.07–56.06% (Table 1, Figure 3). The 5367–5595 protein-coding genes were predicted, of which 4713–4856 genes were classified into 24 functional catalogs in the COG database.

Table 1. Genome features of the *K. oxytoca* isolates of aquatic animal origins.

Genome Feature	*K. oxytoca* Isolate							
	7-7-27	**8-1-12-7**	**8-2-3-6**	**8-2-11**	**8-3-38**	**8-6-19**	**8-8-40**	**8-11-1**
Genome size (bp)	6,018,771	5,896,043	5,837,340	5,927,746	5,942,002	5,878,009	5,905,709	5,851,997
G + C (%)	55.97	56	56.02	55.41	56.06	55.07	55.99	55.98
DNA Scaffold	90	36	46	34	40	74	49	35
Total Predicted Gene	5601	5423	5369	5480	5479	5461	5431	5398
Protein-Coding Gene	5595	5417	5367	5474	5476	5457	5426	5395
RNA Gene	210	238	222	222	224	236	256	207
Genes Assigned to COG	4856	4799	4764	4796	4813	4713	4807	4774
Genes with Unknown Function	80	73	69	32	73	62	85	79
GI	11	12	12	10	19	15	13	13
Prophage	6	3	1	1	4	2	3	4
In	1	0	0	0	0	1	0	0
IS	7	1	0	2	1	4	1	0
CRISPR	12	13	6	7	7	14	10	10

A typical Poisson distribution is shown in the sequencing data, indicating less repetitive DNA in the *K. oxytoca* genomes (Supplementary Materials: Figure S4). The obtained genomes contained 5369–5601 predicted genes, consistent with the 34 *K. oxytoca* strains encoding 4840–6521 predicted genes, whose complete genome sequences (5.39–6.25 Mb) were available in the GenBank database (accessed on 1 October 2023). Of these, only a few were isolated from the environment ($n = 4$). The results of this study enrich the *K. oxytoca* genome database, and fill the prior gap in the genomes of *K. oxytoca* of aquatic animal origins.

The draft genomes of the *K. oxytoca* 7-7-27, 8-1-12-7, 8-2-3-6, 8-2-11, 8-3-38, 8-6-19, 8-8-40, and 8-11-1 isolates were deposited in the GenBank database under accession numbers SAMN37879549 to SAMN37879556.

Strikingly, the *K. oxytoca* genomes carried a large number of putative MGEs, particularly GIs ($n = 105$), and prophages ($n = 24$), which may constitute an important driving force in the shaping and reshuffling of the *K. oxytoca* genome. To the best of our knowledge, reports in the current literature on the GIs and prophages in *K. oxytoca* are rare. Moreover, Ins ($n = 2$) and ISs ($n = 16$) were also found in the *K. oxytoca* isolates.

Additionally, genes of plasmid origin were identified in some contigs of the *K. oxytoca* genomes, suggesting possible HGT via plasmids. Moreover, small plasmid DNA was extracted from all the strains. It will be interesting to determine their sequences and evolution origin in future research.
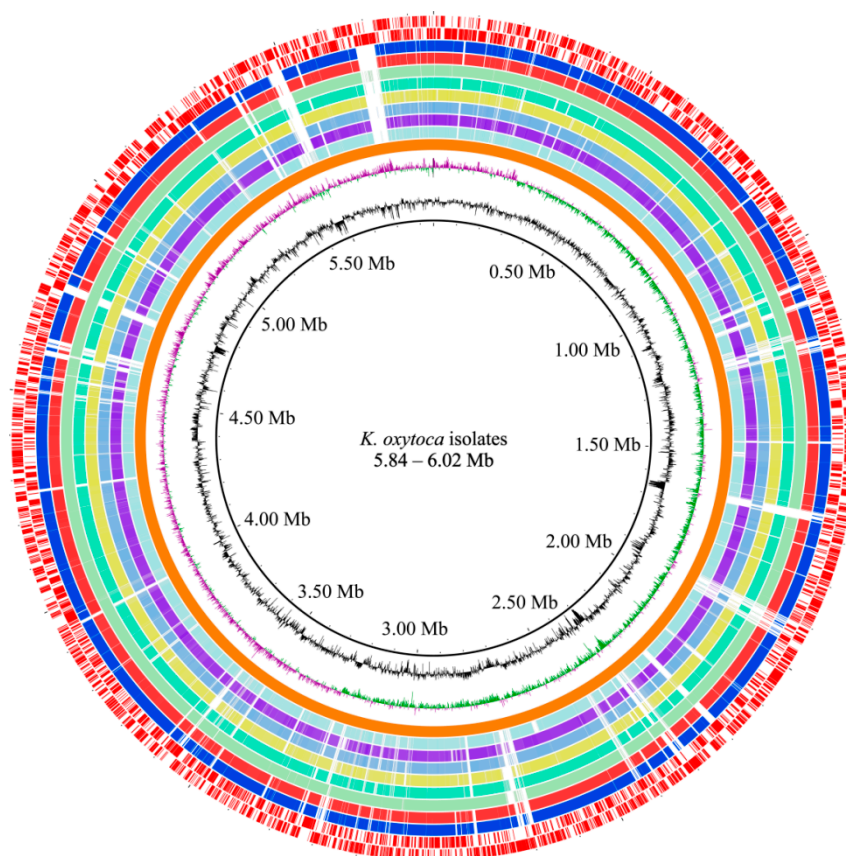
Figure 3. Genome circle map of the eight *K. oxytoca* isolates of aquatic animal origins. Circles from the inside to the outside: the first circle (in black)—GC contents (outward part means higher than average, inward part means lower than average); the second circle—GC-skew (purple value is greater than zero, green value is less than zero); the third circle (in orange)—the reference genome of *K. oxytoca* NCTC13727; the fourth to eleventh circles—*K. oxytoca* 7-7-27, 8-1-12-7, 8-2-3-6, 8-2-11, 8-3-38, 8-6-19, 8-8-40 and 8-11-1 genomes, respectively; and the twelfth to thirteenth circles (in red)—CDSs on the positive and negative chains (inward and outward parts), respectively. The maps were obtained by aligning the sequences of multiple contigs obtained for the individual strains to the genome sequence of the reference strain NCTC13727. The GC content, GC-skew, and marked CDSs were applied to the NCTC13727 strain.

3.5. GIs

GIs are large genomic regions (typically 10–200 Kb) that play a crucial role in bacterial genome evolution. They carry variable genes, such as antibiotic resistance and virulence genes, leading to the generation of hospital 'superbugs', as well as catabolic genes, leading to the formation of new metabolic pathways [26]. In this study, strikingly, a total of 105 GIs were identified in the eight *K. oxytoca* genomes, each of which contained 10–19 GIs in the range of 3328–99,236 bp and carrying 7–81 genes (Supplementary Materials: Figures S5 and S6, Tables S2 and S3). The genome of *K. oxytoca* 8-3-38 originating from *A. granosa* contained the maximum number of GIs ($n = 19$), while that of *K. oxytoca* 8-2-11 from *S. subcrenata* contained the minimum number ($n = 10$).

Interestingly, various function-related genes were identified in the GIs, e.g., virulence, resistance, metabolism, and phage and stress regulation. For example, GI 5 (15,235 bp) of the *K. oxytoca* 8-6-19 genome encoded multidrug efflux-related proteins, e.g., multidrug efflux resistance–nodulation–division (RND) transporter periplasmic adaptor subunit AcrA (*K. oxytoca* 8-6-19_1871), multidrug efflux RND transporter permease subunit AcrB (*K. oxytoca* 8-6-19_1870), and multidrug efflux transporter transcriptional repressor AcrR (*K. oxytoca* 8-6-19_1872). GI 11 (7106 bp) carried nine genes encoding stress-related proteins,

e.g., envelope stress response membrane protein PspB (*K. oxytoca* 8-6-19_4104), envelope stress response membrane protein PspC (*K. oxytoca* 8-6-19_4105), phage shock protein operon transcriptional activator (*K. oxytoca* 8-6-19_4102), phage shock protein PspA (*K. oxytoca* 8-6-19_4103), and phage shock protein PspD (*K. oxytoca* 8-6-19_4106).

Notably, there were 27 identified GIs carrying virulence-related genes in the eight *K. oxytoca* genomes. For example, *K. oxytoca* 8-8-40 contained the maximum number of GIs (GI 1, GI 3, GI 4, GI 7, and GI 8) with virulence-related genes. GI 1 encoded a type II toxin–antitoxin system PemK/MazF family toxin (*K. oxytoca* 8-8-40_0365), and an antitoxin (*K. oxytoca* 8-8-40_0366); GI 3 encoded a type II toxin–antitoxin system RatA family toxin (*K. oxytoca* 8-8-40_1464); GI 4 encoded a type IV toxin–antitoxin system YeeU family antitoxin (*K. oxytoca* 8-8-40_1892), and a TA system toxin CbtA family protein (*K. oxytoca* 8-8-40_1893); GI 7 encoded a toxin YdaT family protein (*K. oxytoca* 8-8-40_2990); GI 8 encoded an inovirus Gp2 family protein (*K. oxytoca* 8-8-40_3456), a virulence factor SrfC family protein (*K. oxytoca* 8-8-40_3464), a virulence factor SrfB (*K. oxytoca* 8-8-40_3465), a type IV toxin-antitoxin system YeeU family antitoxin (*K. oxytoca* 8-8-40_3481), and a TA system toxin CbtA family protein (*K. oxytoca* 8-8-40_3482). Additionally, there were 14 identified GIs carrying T6SS genes, including GI 10 in *K. oxytoca* 7-7-27 genome; GI 6 and GI 7 in *K. oxytoca* 8-1-12-7; GI 8 in *K. oxytoca* 8-2-3-6; GI 3 and GI 4 in *K. oxytoca* 8-8-40; GI 4 and GI 5 in *K. oxytoca* 8-3-38; and GI 3 in *K. oxytoca* 8-11-1.

Additionally, some identified GIs carried phage regulation-related genes in the *K. oxytoca* genomes. For example, GI4 in *K. oxytoca* 8-8-40 encoded an AlpA family phage regulatory protein (*K. oxytoca* 8-8-40_1881), and GI 8 in *K. oxytoca* 8-6-19 encoded a phage regulatory CII family protein (*K. oxytoca* 8-6-19_2771).

3.6. Putative MGEs

3.6.1. Prophages

Prophages are viral genomes integrated into host bacterial genomes. They can confer various phenotypic traits to their hosts, such as enhanced pathogenicity [27]. In this study, a total of 24 prophages were identified in the eight *K. oxytoca* genomes, each of which contained 1–6 prophages (21,338–108,967 bp) carrying 13–71 genes (Supplementary Materials: Figure S7). The predicted prophages contained genetic modules involved in integration/excision, head and tail assembly, cell lysis, DNA modification, and immunity (Supplementary Materials: Tables S4 and S5).

The genome of *K. oxytoca* 7-7-27 from *M. edulis* contained the maximum number of prophage gene clusters (n = 6), which displayed sequence similarity to *Burkholderia*_phage_BcepC6B (42,415 bp, NCBI accession number: NC_005887), *Enterobacter*_phage_HK97 (39,732 bp, NCBI accession number: NC_002167), *Enterobacter*_phage_PsP3 (30,636 bp, NCBI accession number: NC_005340), *Klebsiella*_phage_phiKO2 (51,601 bp, NCBI accession number: NC_005857), Phage_phiO18P (43,101 bp, NCBI accession number: NC_009542), and *Haemophilus*_phage_Aaphi23 (43,033 bp, NCBI accession number: NC_004827), respectively.

The *K. oxytoca* 8-2-3-6 and *K. oxytoca* 8-2-11 genomes contained the minimum number of prophage gene clusters (n = 1), which showed sequence similarity to *Klebsiella*_phage_phiKO2 (51,601 bp, NCBI accession number: NC_005857) and *Enterobacter*_phage_P2 (33,593 bp, NCBI accession number: NC_001895), respectively.

Remarkably, the identified *Klebsiella*_phage_phiKO2 (46,610 bp) in *K. oxytoca* 8-3-38 was also found in the *K. oxytoca* 8-11-1, 7-7-27, 8-2-3-6, 8-8-40, and 8-1-12-7 genomes, with varying length (46,610 bp to 18,994 bp). Similarly, the identified Phage_phiO18P (43,101 bp) in *K. oxytoca* 7-7-27 was also found in *K. oxytoca* 8-6-19, but with a truncated version (27,839 bp). Additionally, the identified *Enterobacter*_phage_ES18 (46,900 bp, NCBI accession number: NC_006949) in *K. oxytoca* 8-8-40 was also present in *K. oxytoca* 8-1-12-7, while the identified *Enterobacter*_phage_P2 (33,593 bp, NCBI accession number: NC_001895) in *K. oxytoca* 8-1-12-7 was found in *K. oxytoca* 8-2-11, as well. These results suggested extensive genome rearrangement during *K. oxytoca* evolution.

Taken together, the identified prophages in the eight *K. oxytoca* genomes were derived from five different genera, including *Burkholderia* spp., *Enterobacter* spp., *Haemophilus* spp., *Klebsiella* spp., and *Pseudomonas* spp., indicating HGT of the phages across different genera and *Klebsiella*. A phylogenetic tree was constructed to show the evolutionary relationship of the identified prophages (Supplementary Materials: Figure S8). Moreover, similar prophages of different sizes, e.g., the identified *Klebsiella*_phage_phiKO2 in the *K. oxytoca* 8-3-38, 8-11-1, 7-7-27, 8-2-3-6, 8-8-40, and 8-1-12-7 genomes and the identified Phage_phiO18P in the *K. oxytoca* 7-7-27 and 8-6-19 genomes, were present in different *K. oxytoca* isolates, suggesting extensive genome rearrangement during *K. oxytoca* evolution. Furthermore, several prophages originating from different genera coexisted in one *K. oxytoca* isolate. For instance, *K. oxytoca* 7-7-27 contained the predicted *Burkholderia*_phage_BcepC6B, *Enterobacter*_phage_HK97, *Enterobacter*_phage_PsP3, *Klebsiella*_phage_phiKO2, *Haemophilus*_phage_Aaphi23, and phage_phiO18P. These results highlighted the considerable compatibility and flexibility of *K. oxytoca* genomes.

3.6.2. Ins

Ins are also genetic hotspots for bacterial genome evolution [28]. They have three essential core features: *intI*, integron-associated recombination site *attI*, and an integron-associated promoter *Pc*. The class 1 Ins are major players in the dissemination of antibiotic resistance genes across pathogens and commensals [29]. In this study, one class 1 In was identified in the *K. oxytoca* 8-6-19 and *K. oxytoca* 7-7-27 genomes, respectively, but absent from the other six genomes (Supplementary Materials: Figure S9 and Table S6).

For instance, the *K. oxytoca* 7-7-27 genome contained a complete In (1815 bp), encoding a trimethoprim-resistant dihydrofolate reductase DfrA14 (*K. oxytoca* 7-7-27_5666) and a class 1 integrase IntI 1 (*K. oxytoca* 7-7-27_5667).

Similarly, the *K. oxytoca* 8-6-19 genome also contained a complete In. However, the total length of the gene cassette array (3365 bp) was larger than that found in the *K. oxytoca* 7-7-27 genome, which encoded a quaternary ammonium compound efflux SMR transporter QacE delta 1 (*K. oxytoca* 8-6-19_5484), an AadA family aminoglycoside 3'-O-nucleotidyltransferase (*K. oxytoca* 8-6-19_5485), a trimethoprim-resistant dihydrofolate reductase DfrA12 (*K. oxytoca* 8-6-19_5486), and a class 1 integrase IntI 1 (*K. oxytoca* 8-6-19_5487).

Acquiring class 1 Ins can enable the development of MDR phenotypes in Gram-negative enterobacteria [30,31]. The results of this study provide additional evidence for this finding, as the *K. oxytoca* 7-7-27 and 8-6-19 isolates were resistant to three and four antibiotics, respectively.

3.6.3. ISs

ISs are the smallest and most numerous autonomous transposable elements in shaping host genomes [32]. In this study, ISs (n = 1 to 7) were found in the *K. oxytoca* 7-7-27, 8-1-12-7, 8-2-11, 8-3-38, 8-6-19, and 8-8-40 genomes, in the range of 594–1448 bp (Supplementary Materials: Table S7).

For example, the *K. oxytoca* 7-7-27 genome contained the maximum number of ISs (n = 7). Notably, the IS (915 bp), belonging to the IS91 family, carried a tyrosine-type DNA invertase (*K. oxytoca* 7-7-27_0499). This IS was also found in the *K. oxytoca* 8-2-11, 8-6-19, and 8-1-12-7 genomes, respectively.

Additionally, the *K. oxytoca* 8-3-38 genome contained only one IS (1114 bp), belonging to the IS5 family, encoding an SDR family oxidoreductase (*K. oxytoca* 8-3-38_3540), suggesting that this IS was a transporter ISs (tIS). The *K. oxytoca* 8-6-19 genome contained four ISs (IS1–IS4), among which the identified IS3 (763 bp) belonged to the IS1-family elements that contained two CDSs for the fusion transposase: the InsA (*K. oxytoca* 8-6-19_5478) for the proximal part of a fusion functional enzyme, and an IS1 family transposase (*K. oxytoca* 8-6-19_5479).

3.7. CRISPR-Cas Arrays

CRISPR-Cas is an adaptive immune system that exists in most bacteria and archaea, preventing them from being infected by foreign genetic elements [33,34]. In this study, a total of 79 CRISPR cassette arrays were identified in the eight *K. oxytoca* genomes; however, none of them contained the Cas protein-encoding gene, suggesting inactive CRISPR-Cas systems in these isolates (Supplementary Materials: Figure S10). Cas is an endonuclease that can cleave foreign DNA, and then, integrate it into the CRISPR array as new spacers [33]. *K. oxytoca* 8-6-19 had the maximum number of CRISPR cassette arrays (*n* = 14), while *K. oxytoca* 8-2-36 had the minimum (*n* = 6). Additionally, different repeated sequences were found in the CRISPR cassette arrays of the *K. oxytoca* genomes. These results provide indirect evidence for an inactive adaptive immunity system but possible active HGT in *K. oxytoca* isolates.

3.8. Strain-Specific Genes of the K. oxytoca Isolates of Aquatic Animal Origins

Approximately 4295 core genes were identified in the eight *K. oxytoca* genomes, which accounted for 74.3% of the pan genes (*n* = 5778). Meanwhile, many strain-specific genes (*n* = 10–403) were identified in the *K. oxytoca* genomes (Figure 4).
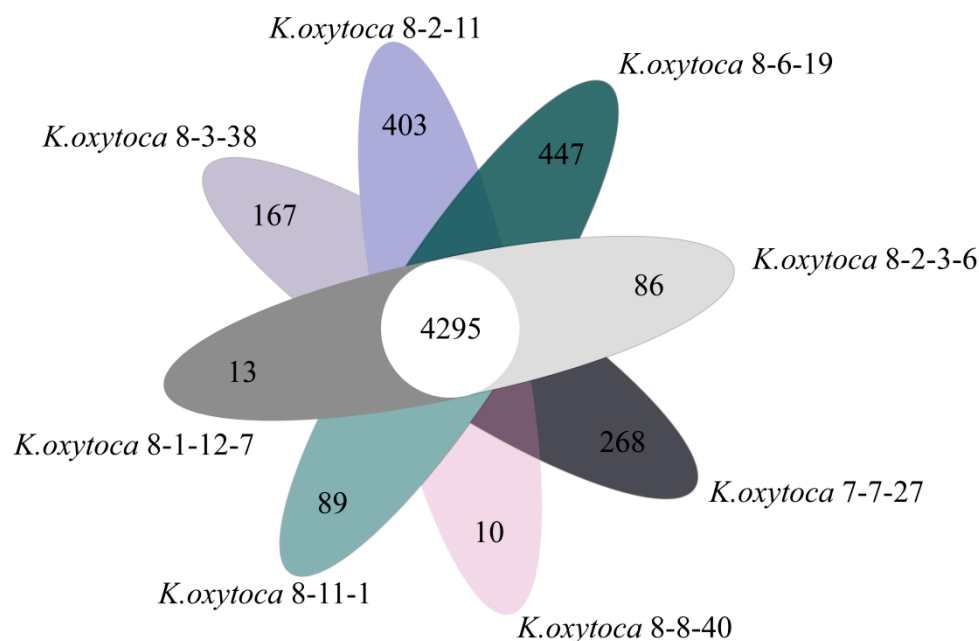

Figure 4. Venn diagram showing the core genes and strain-specific genes in the eight *K. oxytoca* genomes.

The genome of *K. oxytoca* 8-2-11 from *S. subcrenata* harbored the maximum number of strain-specific genes (*n* = 403), whereas *K. oxytoca* 8-8-40 from *A. woodiana* had the minimum (*n* = 10). Notably, approximately 30.0–86.5% of the strain-specific genes encoded hypothetical proteins with unknown proteins in the current databases. These results provide additional genome-level evidence for the genome diversity of *K. oxytoca* isolates of aquatic animal origins.

3.9. Putative Virulence-Associated Genes in the K. oxytoca Genomes

K. oxytoca is associated with human diseases [35]. Nevertheless, few studies are currently available on the virulence of *K. oxytoca* of aquatic animal origins. In this study, based on the obtained *K. oxytoca* genomes, comparative genomic analysis revealed putative virulence-related genes (*n* = 97–104) in the eight *K. oxytoca* genomes (Supplementary Materials: Table S8). *K. oxytoca* 8-3-38 from *A. granosa* contained the maximum number of such genes (*n* = 104).

For example, the virulence-related *fimABCDEFGHI*, *entABCDEFS*, and *mrkABCDFHJ* gene clusters were present in all the *K. oxytoca* genomes. The former is involved in the adhesion and colonization of *K. oxytoca* [36], while the latter two mediate biofilm formation upon biotic and abiotic surfaces [36]. The *K. oxytoca* 8-2-11 and 8-6-19 genomes also contained the *allABCDRS* gene cluster, which provides a nitrogen source to increase the virulence of bacteria at infection sites [37]. Specifically, the *sciN/tssJ* gene was only found in the *K. oxytoca* 8-3-38 and 8-11-1 genomes, while the *ureA* and *dotU/tssL* genes were present in the *K. oxytoca* 8-2-11 and 8-3-38 genomes, respectively.

Additionally, the *RelE*, *SymE*, and *IlpA* genes, which are involved in adhesion, colonization, the secretion system, and gene regulation, were also identified in the eight isolates of aquatic animal origins. For example, the RelE protein in *Escherichia colicytotoxin* exhibited ribosome-binding activity in vitro, suggesting that it is an inhibitor of translation [38], while the overproduction of SymE in *E. coli* led to cell growth inhibition, decreased protein synthesis, and increased RNA degradation [39]. IlpA was an adhesion and immune stimulator [40], while *mrkA* gene expression was related to biofilm formation in carbapenemase-producing *K. pneumoniae* [41]. The periodontal disease-associated bacterium *Porphyromonas gingivalis* primarily uses FimA fimbriae for adhesion to and colonization in the gingival tissues. FimC, FimD, and FimE were associated with the fimbriae as minor components [42]. The potential virulence-related genes may be candidate targets for the development of new diagnostics, vaccines, and treatments to control *K. oxytoca* infection. It will be interesting to investigate their potential virulence using cell and animal models in future research.

3.10. Antibiotic and Heavy Metal Resistance-Associated Genes in the K. oxytoca Genomes and Their Bacterial Resistance Phenotypes

The increasing prevalence of infections caused by MDR pathogens poses a serious threat to global public health and places a heavy burden on health-care systems [43]. In this study, comparative genomic analysis also revealed putative antibiotic resistance-related genes (n = 27–62) in the *K. oxytoca* genomes (Supplementary Materials: Table S9), e.g., *arcABDEF*, *aph3-1*, *arnAC*, *bacA*, *baeRS*, *blaOXY*, *cpxA*, *crp*, *emrABR*, *eptA*, *kdpE*, *marA*, *mdfA*, *mdtABCGHIJMN*, *msbA*, *nmpC*, *ompCN*, *oqxAB*, *phoE*, *ramA*, *sdiA*, *soxR*, *tolC*, *ugd*, and *yojI*, which are involved in resistance to cephalosporin, fluoroquinolone, tetracycline (TET), aminoglycoside, macrolide, phenicol, sulfonamide, rifamycin, and fosfomycin. *K. oxytoca* 7-7-27 contained the maximum number of such genes (n = 62), whereas *K. oxytoca* 8-2-3-6 and 8-3-38 isolates had the fewest (n = 27).

For instance, the multidrug-effluxing or transporter-related genes were found in all the *K. oxytoca* genomes, e.g., membrane fusion protein of RND family multidrug efflux pump (*acrA*), multidrug efflux RND transporter permease subunit AcrB (*acrB*), multidrug efflux RND transporter permease AcrD (*acrD*), efflux RND transporter periplasmic adaptor subunit (*acrE*), efflux RND transporter permease subunit (*acrF*), multidrug ABC transporter permease/ATP-binding protein (*yojI*), lipid A ABC transporter ATP-binding protein/permease MsbA (*msbA*), MFS transporter (*mdfA*), phosphoethanolamine transferase EptA (*mptA*), cAMP-activated global transcriptional regulator CRP (*crp*), efflux RND transporter periplasmic adaptor subunit (*oqxA*), multidrug efflux RND transporter permease subunit OqxB (*oqxB*), multidrug efflux MFS transporter permease subunit EmrB (*emrB*), multidrug efflux MFS transporter periplasmic adaptor subunit EmrA (*emrA*), and transcriptional repressor MprA (*emrR*).

The multiple efflux transporter transcriptional reporter *AcrR* gene was found in the *K. oxytoca* 7-7-27, 8-2-11, 8-1-12-7, and 8-11-1 genomes, while the *aadA*, *ebr*, and *dfrA12* genes were present in *K. oxytoca* 8-6-19, which encoded AadA family aminoglycoside 3″-O-nucleotidyltransferase, quaternary ammonium compound efflux SMR transporter QacE delta 1, and trimethoprim-resistant dihydrofolate reductase DfrA12, respectively.

Additionally, the *aadA*, *ebr*, and *dfrA12* genes encoded AadA family aminoglycoside 3′-O-nucleotidyltransferase, quaternary ammonium compound efflux SMR transporter QacE delta 1, and trimethoprim-resistant dihydrofolate reductase DfrA12, respectively,

which confer resistance to aminoglycoside [44], cephalosporin [45], and trimethoprim [46], respectively. Notably, *K. oxytoca* 7-7-27 from *M. edulis* contained the maximum number of such genes (*n* = 62), suggesting antibiotic exposure risk of its host *M. edulis.*

Heavy metal tolerance-related genes were also identified in some GIs in the *K. oxytoca* genomes as well. For example, the *kdpE* gene, encoding a transcriptional activator that is part of the two-component system KdpD/KdpE, was found in all the *K. oxytoca* isolates. KdpE has been identified as an adaptive regulator involved in the potassium transport, virulence, and intracellular survival of pathogenic bacteria [47].

To confirm the in silico predicted resistance genes, the resistance phenotypes of the *K. oxytoca* isolates were examined experimentally. The results revealed that the *K. oxytoca* isolates harbored different antibiotic resistance profiles (Table S1). For instance, three isolates displayed MDR phenotypes: *K. oxytoca* 8-6-19 isolated from *N. cumingi Crosse* was resistant to chloramphenicol (CHL), sulphamethoxazole-trimethoprim (SXT), kanamycin (KAN), and TET; *K. oxytoca* 7-7-27 from *M. edulis* to CHL, SXT, and TET; and *K. oxytoca* 8-11-1 from *C. auratus* to CIP, norfloxacin (NOR), and SXT. Meanwhile, the *K. oxytoca* isolates also displayed different heavy metal tolerance profiles. For instance, *K. oxytoca* 8-8-40 from *A. woodiana* and *K. oxytoca* 8-2-11 from *S. subcrenata* were tolerant to the maximum number of heavy metal ions evaluated in this study: $Cd^{2+}/Cr^{3+}/Cu^{2+}/Hg^{2+}/Pb^{2+}/Zn^{2+}$ and $Cr^{3+}/Cu^{2+}/Hg^{2+}/Mn^{2+}/Pb^{2+}/Zn^{2+}$, respectively.

3.11. Phylogenetic Relatedness of the K. oxytoca Isolates of Aquatic Animal Origins

Based on the eight *K. oxytoca* genomes obtained in this study, we constructed a phylogenetic tree, combined with 34 *K. oxytoca* strains, whose complete genome sequences are currently available in the GenBank database (Supplementary Materials: Table S10). The majority of these *K. oxytoca* strains (*n* = 27) were isolated from human specimens, while only a few were isolated from the environment (*n* = 4) and the other sources (*n* = 3), from the period of 1980–2022. Seven different clusters, designated as Clusters A–G, were classified (Figure 5).
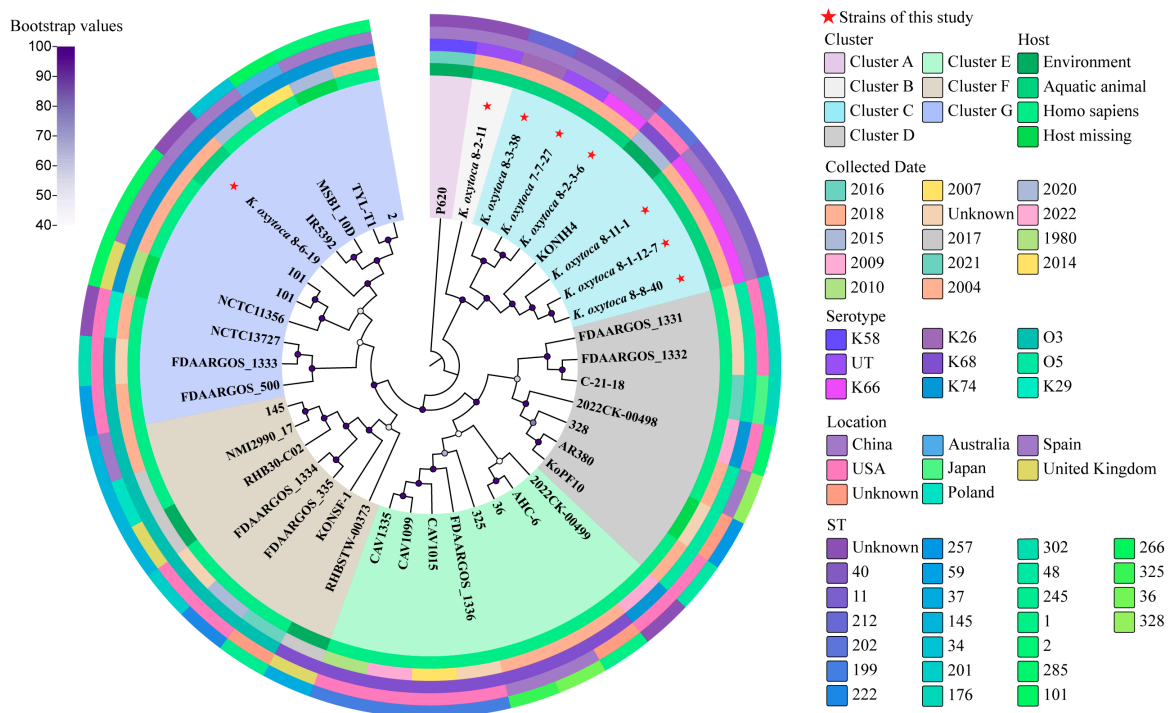

Figure 5. A phylogenetic tree showing the relationships of the 42 *K. oxytoca* genomes. Complete genome sequences of the 34 *K. oxytoca* isolates were retrieved from the GenBank database, with accession numbers shown in Table S10. The sequenced *K. oxytoca* genomes in this study are marked

with red stars. The maximum likelihood method was used to build the tree, with 1000 bootstrap replications and a cut-off threshold of ≥50% bootstrap values.

K. oxytoca 7-7-27, 8-1-12-7, 8-2-3-6, 8-3-38, 8-8-40, and 8-11-1 isolates, originating from *M. edulis*, *P. clarkii*, *S. constricta*, *A. granosa*, *A. woodiana* and *C. auratus*, respectively, fell into Cluster C, together with *K. oxytoca* KONIH4 (GenBank accession no. NZ_CP026269.1), which was isolated from waste water in 2015 in the USA.

K. oxytoca 8-2-11 from *S. subcrenata* was classified into a single Cluster (B), while *K. oxytoca* 8-6-19 from *N. cumingi Crosse* was grouped into Cluster G, together with the other ten *K. oxytoca* strains, but showed the closest phylogenetic distance to the *K. oxytoca* strain (GenBank accession no. NZ_CP064108.1), which was isolated from a human specimen in 2015 in China. Notably, *K. oxytoca* 8-6-19 was phylogenetically distant from the other seven *K. oxytoca* isolates of aquatic animal origins.

3.12. MLST of the K. oxytoca Isolates of Aquatic Animal Origins

The MLST analysis against the MLST database revealed that *K. oxytoca* 7-7-27, 8-1-12-7, 8-3-38, 8-8-40, and 8-11-1 isolates belonged to ST-40, ST-11, ST-212, ST-11, and ST-11, respectively, while *K. oxytoca* 8-2-3-6, 8-2-11, and 8-6-19 isolates were new STs, which have not been classified so far.

4. Conclusions

K. oxytoca is an emerging pathogen that can cause life-threatening infectious diseases in humans. Recently, we reported for the first time the presence of *K. oxytoca* in edible aquatic animals sampled in Shanghai and Fuzhou, China, in July–September of 2018–2019. In this study, we further investigated the environmental fitness and genome evolution signatures of such *K. oxytoca* isolates ($n = 8$), which originated from six species of crustaceans, one species of shellfish, and one species of fish. The results revealed that the *K. oxytoca* isolates were capable of growing under a broad spectrum of environmental conditions (pH 4.5–8.5, 0.5–6.5% NaCl) in TSB at 37 °C, indicating their remarkable compatibility and fitness in their niches. Among the isolates, *K. oxytoca* 8-2-11 from *S. subcrenata* showed the strongest capability to form a biofilm, while *K. oxytoca* 8-3-38 from *A. granosa* displayed the fastest swimming mobility.

The genome sequences of the eight *K. oxytoca* isolates were determined (5.84–6.02 Mb, 55.07–56.06% GC content), which contained 5367–5595 protein-encoding genes. Strikingly, numerous putative MGEs, particularly GIs ($n = 105$), and prophages ($n = 24$), were for the first time found in the *K. oxytoca* genomes, which provided the bacterium with specific adaptation traits, such as resistance, virulence, and material metabolism. Interestingly, the identified prophage homologues were derived from *Burkholderia* spp., *Enterobacter* spp., *Klebsiella* spp., *Pseudomonas* spp., and *Haemophilus* spp., suggesting phage transmission across *Klebsiella* and the other four genera. Moreover, some prophage homologues, such as the *Klebsiella*_phage_phiKO2, *Enterobacter*_phage_ES18, *Enterobacter*_phage_P2, and Phage_phiO18P, were found in different *K. oxytoca* genomes. Notably, several prophage homologues originating from different genera co-existed in one *K. oxytoca* isolate. CRISPR cassette arrays ($n = 75$) were also identified in the eight *K. oxytoca* genomes. However, no Cas protein-encoding gene was found, which provided indirect evidence for an inactive adaptive immunity system but possible active HGT in the *K. oxytoca* isolates. These results indicate considerable compatibility and flexibility of the bacterial genomes.

Comparative genomic analyses also revealed many ARGs ($n = 27$–62) and virulence ($n = 97$–104)-related genes in the *K. oxytoca* genomes. *K. oxytoca* 7-7-27 from *M. edulis* contained the highest number of ARGs ($n = 97$), while *K. oxytoca* 8-3-38 carried the most virulence-related genes ($n = 104$). These genes may be candidate targets for the development of new diagnostics, vaccines, and treatments to control *K. oxytoca* infection. In addition, numerous strain-specific ($n = 10$–447) genes were also present in the *K. oxytoca* genomes, approximately 30.0–86.5% of which encoded unknown proteins. *K. oxytoca* 8-6-19 from *N.*

cumingi Crosse contained the highest number of strain-specific genes (*n* = 447), whereas *K. oxytoca* 8-8-40 from *A. woodiana* had the fewest (*n* = 10).

Overall, the results of this study enrich the *K. oxytoca* genome database and fill prior gaps in *K. oxytoca* genomes of aquatic animal origins, and also demonstrate for the first time the environmental compatibility and genome flexibility of *K. oxytoca* isolates.

Supplementary Materials: The following supporting information can be downloaded at: https://www.mdpi.com/article/10.3390/d16010030/s1. Table S1: The resistance phenotypes of the *K. oxytoca* isolates used in this study; Table S2: The identified GIs in the *K. oxytoca* genomes; Table S3: The predicted genes in the identified GIs in the *K. oxytoca* genomes; Table S4: The identified prophages in the *K. oxytoca* genomes; Table S5: The predicted genes in the identified prophages in the *K. oxytoca* genomes; Table S6: The identified Ins in the *K. oxytoca* genomes; Table S7: The identified ISs in the *K. oxytoca* genomes; Table S8: The putative virulence-related genes identified in the *K. oxytoca* genomes; Table S9: The putative antibiotic and heavy metal resistance-related genes identified in the *K. oxytoca* genomes; Table S10: The thirty-four *K. oxytoca* strains with complete genomes used in the phylogenetic tree. Figure S1: Growth curves of the *K. oxytoca* isolates of aquatic animal origins under different concentrations of NaCl. A-H: *K. oxytoca* 7-7-27, 8-1-12-7, 8-2-3-6, 8-2-11, 8-3-38, 8-6-19, 8-8-40, and 8-11-1 isolates were incubated in the TSB (pH 7.2, 0.5–8.5% NaCl) at 37 °C for 24 h, respectively. Figure S2: Growth curves of the *K. oxytoca* isolates of aquatic animal origins under different pH conditions. A–H: *K. oxytoca* 7-7-27, 8-1-12-7, 8-2-3-6, 8-2-11, 8-3-38, 8-6-19, 8-8-40, and 8-11-1 isolates were incubated in the TSB (0.5% NaCl, pH 3.5–8.5) at 37 °C for 24 h, respectively. Figure S3: The swimming loops of the *K. oxytoca* isolates of aquatic animal origins. The *K. oxytoca* 7-7-27, 8-1-12-7, 8-2-3-6, 8-2-11, 8-3-38, 8-6-19, 8-8-40, and 8-11-1 isolates were incubated in the TSB (0.5% NaCl, pH 8.5, 0.25% agar) at 37 °C for 72 h. Figure S4: The k-mer analysis for *K. oxytoca* sequencing reads based on the number of unique 17-mers. A–H: *K. oxytoca* 7-7-27, 8-1-12-7, 8-2-3-6, 8-2-11, 8-3-38, 8-6-19, 8-8-40, and 8-11-1 genomes, respectively. Figure S5: Gene organizations of the GIs identified in the *K. oxytoca* genomes (A–C). Different colors refer to COG classification to mark gene functions (Figure S6). Figure S6: The COG function classification of the genes in the putative MGEs. Figure S7: Gene organizations of the prophages identified in the *K. oxytoca* genomes. Different colors refer to COG classification to mark gene functions (Figure S6). Figure S8: Phylogenetic relationship of the identified prophages in the *K. oxytoca* genomes. Figure S9: A structure diagram of the Ins identified in the *K. oxytoca* genomes. Figure S10: Structural features of the CRISPR cassette arrays identified in the *K. oxytoca* genomes. The repeat sequences are shown as rectangles in different colors, and the spacer regions are represented by rhombuses in different colors.

Author Contributions: S.S.: investigation, data curation, and writing—original draft preparation; T.G.: data analysis and writing—original draft preparation; Y.O.: writing—original draft preparation; Y.W. and L.X.: discussion and supervision; L.C.: funding acquisition, conceptualization, and writing—review and editing. All authors have read and agreed to the published version of the manuscript.

Institutional Review Board Statement: Not applicable.

Informed Consent Statement: Not applicable.

Data Availability Statement: Draft genome sequences of the seven *K. oxytoca* isolates were deposited in the GenBank database under accession numbers SAMN37879549—SAMN37879556.

Conflicts of Interest: The authors declare no conflicts of interest.

References

1. Power, J.T.; Calder, M.A. Pathogenic significance of *Klebsiella oxytoca* in acute respiratory tract infection. *Thorax* **1983**, *38*, 205–208. [CrossRef] [PubMed]
2. Herzog, K.A.; Schneditz, G.; Leitner, E.; Feierl, G.; Hoffmann, K.M.; Zollner-Schwetz, I.; Krause, R.; Gorkiewicz, G.; Zechner, E.L.; Högenauer, C. Genotypes of *Klebsiella oxytoca* isolates from patients with nosocomial pneumonia are distinct from those of isolates from patients with antibiotic-associated hemorrhagic colitis. *J. Clin. Microbiol.* **2014**, *52*, 1607–1616. [CrossRef] [PubMed]
3. Soto-Hernández, J.L.; Soto-Ramírez, A.; Pérez-Neri, I.; Angeles-Morales, V.; Cárdenas, G.; Barradas, V.A. Multidrug-resistant *Klebsiella oxytoca* ventriculitis, successfully treated with intraventricular tigecycline: A case report. *Clin. Neurol. Neurosurg.* **2020**, *188*, 105592. [CrossRef] [PubMed]
4. Dago, T.R.; Zewudie, A.; Mamo, Y.; Feyissa, D.; Geleta, S. Multi-drug resistant post corneal repair *Klebsiella oxytoca's* keratitis. *Int. Med. Case. Rep. J.* **2020**, *13*, 537–541. [CrossRef] [PubMed]
5. Högenauer, C.; Langner, C.; Beubler, E.; Lippe, I.T.; Schicho, R.; Gorkiewicz, G.; Krause, R.; Gerstgrasser, N.; Krejs, G.J.; Hinterleitner, T.A. *Klebsiella oxytoca* as a causative organism of antibiotic-associated hemorrhagic colitis. *N. Engl. J. Med.* **2006**, *355*, 2418–2426. [CrossRef] [PubMed]
6. Paveglio, S.; Ledala, N.; Rezaul, K.; Lin, Q.; Zhou, Y.; Provatas, A.A.; Bennett, E.; Lindberg, T.; Caimano, M.; Matson, A.P. Cytotoxin-producing *Klebsiella oxytoca* in the preterm gut and its association with necrotizing enterocolitis. *Emerg. Microbes. Infect.* **2020**, *9*, 1321–1329. [CrossRef] [PubMed]
7. Lin, T.C.; Hung, Y.P.; Lin, W.T.; Dai, W.; Huang, Y.L.; Ko, W.C. Risk factors and clinical impact of bacteremia due to carbapenem-nonsusceptible Enterobacteriaceae: A multicenter study in southern Taiwan. *J. Microbiol. Immunol. Infect.* **2021**, *54*, 1122–1129. [CrossRef] [PubMed]
8. Carrie, C.; Walewski, V.; Levy, C.; Alexandre, C.; Baleine, J.; Charreton, C.; Coche-Monier, B.; Caeymaex, L.; Lageix, F.; Lorrot, M.; et al. *Klebsiella pneumoniae* and *Klebsiella oxytoca* meningitis in infants. Epidemiological and clinical features. *Arch. Pediatr.* **2019**, *26*, 12–15. [CrossRef]
9. Sabio, J.M.; López-Gómez, M.; Jiménez-Alonso, J. Spontaneous spondylodiscitis caused by *Klebsiella oxytoca*. *Ann. Rheum. Dis.* **2002**, *61*, 758–759. [CrossRef]
10. Surani, A.; Slama, E.M.; Thomas, S.; Ross, R.W.; Cunningham, S.C. *Raoultella ornithinolytica* and *Klebsiella oxytoca* pyogenic liver abscess presenting as chronic cough. *IDCases* **2020**, *20*, e00736. [CrossRef]
11. Gharavi, M.J.; Zarei, J.; Roshani-Asl, P.; Yazdanyar, Z.; Sharif, M.; Rashidi, N. Comprehensive study of antimicrobial susceptibility pattern and extended spectrum beta-lactamase (ESBL) prevalence in bacteria isolated from urine samples. *Sci. Rep.* **2021**, *11*, 578. [CrossRef] [PubMed]
12. Yahya Abdulla, N.; Abduljabbar Jaloob Aljanaby, I.; Hayder Hasan, T.; Abduljabbar Jaloob Aljanaby, A. Assessment of ß-lactams and carbapenems antimicrobials resistance in *Klebsiella oxytoca* isolated from patients with urinary tract infections in Najaf, Iraq. *Arch. Razi. Inst.* **2022**, *77*, 669–673. [CrossRef] [PubMed]
13. Yang, J.; Long, H.; Hu, Y.; Feng, Y.; McNally, A.; Zong, Z. *Klebsiella oxytoca* complex: Update on taxonomy, antimicrobial resistance, and virulence. *Clin. Microbiol. Rev.* **2022**, *35*, e0000621. [CrossRef] [PubMed]
14. Abdurehman Damissie, A.; Abdurahman Musa, K. Isolation, assessments of risk factors, and antimicrobial susceptibility test of *Klebsiella* from gut of bee in and around Haramaya University bee farm, East Hararghe, Oromia regional state, Ethiopia. *Vet. Med. Int.* **2022**, *2022*, 9460543. [CrossRef]
15. Ni, L.; Xu, Y.; Chen, L. First experimental evidence for the presence of potentially virulent *Klebsiella oxytoca* in 14 species of commonly consumed aquatic animals, and phenotyping and genotyping of *K. oxytoca* isolates. *Antibiotics* **2021**, *10*, 1235. [CrossRef] [PubMed]
16. Singh, L.; Cariappa, M.P.; Kaur, M. *Klebsiella oxytoca*: An emerging pathogen? *Med. J. Armed. Forces. India.* **2016**, *72*, S59–S61. [CrossRef] [PubMed]
17. Kunhikannan, S.; Thomas, C.J.; Franks, A.E.; Mahadevaiah, S.; Kumar, S.; Petrovski, S. Environmental hotspots for antibiotic resistance genes. *Microbiology Open* **2021**, *10*, e1197. [CrossRef] [PubMed]
18. Guan, H.; Xie, L.; Chen, L. Survival and genome evolution signatures of *Klebsiella pneumoniae* isolates originated in seven species of aquatic animals. *Diversity* **2023**, *15*, 527. [CrossRef]
19. Pal, A.; Bhattacharjee, S.; Saha, J.; Sarkar, M.; Mandal, P. Bacterial survival strategies and responses under heavy metal stress: A comprehensive overview. *Crit. Rev. Microbiol.* **2022**, *48*, 327–355. [CrossRef]
20. Xu, Y.; Ni, L.; Guan, H.; Chen, D.; Qin, S.; Chen, L. First report of potentially pathogenic *Klebsiella pneumoniae* from serotype K2 in mollusk *Tegillarca granosa* and genetic diversity of *Klebsiella pneumoniae* in 14 species of edible aquatic animals. *Foods* **2022**, *11*, 4058. [CrossRef]
21. Chen, D.; Li, X.; Ni, L.; Xu, D.; Xu, Y.; Ding, Y.; Xie, L.; Chen, L. First experimental evidence for the presence of potentially toxic *Vibrio cholerae* in snails, and virulence, cross-resistance and genetic diversity of the bacterium in 36 species of aquatic food animals. *Antibiotics* **2021**, *10*, 412. [CrossRef] [PubMed]

22. Xu, D.; Peng, X.; Xie, L.; Chen, L. Survival and genome diversity of *Vibrio parahaemolyticus* isolated from edible aquatic animals. *Diversity* **2022**, *14*, 350. [CrossRef]
23. Yang, L.; Wang, Y.; Yu, P.; Ren, S.; Zhu, Z.; Jin, Y.; Yan, J.; Peng, X.; Chen, L. Prophage-related gene VpaChn25_0724 contributes to cell membrane integrity and growth of *Vibrio parahaemolyticus* CHN25. *Front. Cell. Infect. Microbiol.* **2020**, *10*, 595709. [CrossRef] [PubMed]
24. Hall-Stoodley, L.; Costerton, J.W.; Stoodley, P. Bacterial biofilms: From the natural environment to infectious diseases. *Nat. Rev. Microbiol.* **2004**, *2*, 95–108. [CrossRef] [PubMed]
25. Josenhans, C.; Suerbaum, S. The role of motility as a virulence factor in bacteria. *Int. J. Med. Microbiol.* **2002**, *291*, 605–614. [CrossRef] [PubMed]
26. Langille, M.G.; Hsiao, W.W.; Brinkman, F.S. Detecting genomic islands using bioinformatics approaches. *Nat. Rev. Microbiol.* **2010**, *8*, 373–382. [CrossRef] [PubMed]
27. Rezaei Javan, R.; Ramos-Sevillano, E.; Akter, A.; Brown, J.; Brueggemann, A.B. Prophages and satellite prophages are widespread in *Streptococcus* and may play a role in pneumococcal pathogenesis. *Nat. Commun.* **2019**, *10*, 4852. [CrossRef]
28. Engelstädter, J.; Harms, K.; Johnsen, P.J. The evolutionary dynamics of integrons in changing environments. *ISME J.* **2016**, *10*, 1296–1307. [CrossRef]
29. Sabbagh, P.; Rajabnia, M.; Maali, A.; Ferdosi-Shahandashti, E. Integron and its role in antimicrobial resistance: A literature review on some bacterial pathogens. *Iran. J. Basic. Med. Sci.* **2021**, *24*, 136–142. [CrossRef]
30. Ahmadian, L.; Haghshenas, M.R.; Mirzaei, B.; Bazgir, Z.N.; Goli, H.R. Distribution and molecular characterization of resistance gene cassettes containing class 1 integrons in multi-drug resistant (MDR) clinical isolates of *Pseudomonas aeruginosa*. *Infect. Drug. Resist.* **2020**, *13*, 2773–2781. [CrossRef]
31. Ghaly, T.M.; Chow, L.; Asher, A.J.; Waldron, L.S.; Gillings, M.R. Evolution of class 1 integrons: Mobilization and dispersal via food-borne bacteria. *PLoS ONE* **2017**, *12*, e0179169. [CrossRef] [PubMed]
32. Patricia, S.; Edith, G.; Mick, C. Bacterial insertion sequences: Their genomic impact and diversity. *FEMS Microbiol. Rev.* **2015**, *38*, 865–891. [CrossRef]
33. Deveau, H.; Garneau, J.E.; Moineau, S. CRISPR/Cas system and its role in phage-bacteria interactions. *Annu. Rev. Microbiol.* **2010**, *64*, 475–493. [CrossRef] [PubMed]
34. Horvath, P.; Barrangou, R. CRISPR/Cas, the immune system of bacteria and archaea. *Science* **2010**, *327*, 167–170. [CrossRef] [PubMed]
35. Iwadare, T.; Kimura, T.; Sugiura, A.; Takei, R.; Kamakura, M.; Wakabayashi, S.I.; Okumura, T.; Hara, D.; Nakamura, A.; Umemura, T. Pyogenic liver abscess associated with *Klebsiella oxytoca*: Mimicking invasive liver abscess syndrome. *Heliyon* **2023**, *9*, e21537. [CrossRef] [PubMed]
36. Araújo, B.F.; Ferreira, M.L.; Campos, P.A.; Royer, S.; Gonçalves, I.R.; da Fonseca Batistão, D.W.; Fernandes, M.R.; Cerdeira, L.T.; Brito, C.S.; Lincopan, N.; et al. Hypervirulence and biofilm production in KPC-2-producing *Klebsiella pneumoniae* CG258 isolated in Brazil. *J. Med. Microbiol.* **2018**, *67*, 523–528. [CrossRef] [PubMed]
37. Arena, F.; Henrici De Angelis, L.; Pieralli, F.; Di Pilato, V.; Giani, T.; Torricelli, F.; D'Andrea, M.M.; Rossolini, G.M. Draft genome sequence of the first hypermucoviscous *Klebsiella quasipneumoniae* subsp. *quasipneumoniae* isolate from a bloodstream infection. *Genome Announc.* **2015**, *3*, e00952-15. [CrossRef]
38. Galvani, C.; Terry, J.; Ishiguro, E.E. Purification of the RelB and RelE proteins of *Escherichia coli*: RelE binds to RelB and to ribosomes. *J. Bacteriol.* **2001**, *183*, 2700–2703. [CrossRef]
39. Kawano, M.; Aravind, L.; Storz, G. An antisense RNA controls synthesis of an SOS-induced toxin evolved from an antitoxin. *Mol. Microbiol.* **2007**, *64*, 738–754. [CrossRef]
40. Zheng, H.Y.; Yan, L.; Yang, C.; Wu, Y.R.; Qin, J.L.; Hao, T.Y.; Yang, D.J.; Guo, Y.C.; Pei, X.Y.; Zhao, T.Y.; et al. Population genomics study of *Vibrio alginolyticus*. *Hereditas* **2021**, *43*, 350–361. [CrossRef]
41. Gual-de-Torrella, A.; Delgado-Valverde, M.; Pérez-Palacios, P.; Oteo-Iglesias, J.; Rojo-Molinero, E.; Macià, M.D.; Oliver, A.; Pascual, Á.; Fernández-Cuenca, F. Prevalence of the fimbrial operon mrkABCD, mrkA expression, biofilm formation and effect of biocides on biofilm formation in carbapenemase-producing *Klebsiella pneumoniae* isolates belonging or not belonging to high-risk clones. *Int. J. Antimicrob. Agents* **2022**, *60*, 106663. [CrossRef] [PubMed]
42. Nagano, K. FimA fimbriae of the periodontal disease-associated bacterium *Porphyromonas gingivalis*. *Yakugaku Zasshi* **2013**, *133*, 963–974. [CrossRef] [PubMed]
43. Cerceo, E.; Deitelzweig, S.B.; Sherman, B.M.; Amin, A.N. Multidrug-resistant gram-negative bacterial infections in the hospital setting: Overview, implications for clinical practice, and emerging treatment options. *Microb. Drug. Resist.* **2016**, *22*, 412–431. [CrossRef] [PubMed]
44. Frank, K.L.; Bundle, S.F.; Kresge, M.E.; Eggers, C.H.; Samuels, D.S. aadA confers streptomycin resistance in *Borrelia burgdorferi*. *J. Bacteriol.* **2003**, *185*, 6723–6727. [CrossRef] [PubMed]
45. Li, P.; Lei, T.; Zhou, Y.; Dai, Y.; Yang, Z.; Luo, H. EBR-5, a novel variant of metallo-β-lactamase EBR from multidrug-resistant *Empedobacter stercoris*. *Microbiol. Spectr.* **2023**, *12*, e0003923. [CrossRef]

46. Sadek, M.; Poirel, L.; Nordmann, P.; Nariya, H.; Shimamoto, T.; Shimamoto, T. Draft genome sequence of an mcr-1/IncI2-carrying multidrug-resistant *Escherichia coli* B1:ST101 isolated from meat and meat products in Egypt. *J. Glob. Antimicrob. Resist.* **2020**, *20*, 41–42. [CrossRef]
47. Freeman, Z.N.; Dorus, S.; Waterfield, N.R. The KdpD/KdpE two-component system: Integrating K$^+$ homeostasis and virulence. *PLoS Pathog.* **2013**, *9*, e1003201. [CrossRef]